Abnormal Effects of Cations (Li+, Na+, and K+) on Photoelectrochemical and Electrocatalytic Water Splitting

Chunmei Ding, Xin Zhou, Jingying Shi, Pengli Yan, Zhiliang Wang, Guiji Liu, and Can Li*

State Key Laboratory of Catalysis, Dalian Institute of Chemical Physics, Chinese Academy of Sciences, Dalian National Laboratory for Clean Energy, Dalian 116023, China

Ⓢ Supporting Information

ABSTRACT: The electrode−electrolyte interface chemistry is highly important for photoelectrochemical (PEC) and electrocatalytic water splitting where cations in the electrolyte are often crucial. However, the roles of cations in an electrolyte are much debated and not well-understood. This work reports that the PEC and electrocatalytic water oxidation (WO) activities in basic electrolytes with different cations follow an unexpected trend (Li+ > K+ > Na+) especially for long-term reaction. Such an abnormal order of activity is found to be the balance effect of two factors: the distinct extents of the weakening of O−H bond on electrode surface after interacting with cations in different electrolytes and the different rates of oxygen reduction reaction (ORR) which turns out to be dominant. Li+ not only brings the most significant decrease of O−H bond strength but also is most effective for avoiding back reaction, while Na+ shows the most detrimental effect on WO because of ORR. Our results provide important insight into the roles of cations in WO and demonstrate a new strategy of tailoring the electrode−electrolyte interface via judicious choice of cations in electrolyte for more efficient PEC and electrocatalytic water splitting.
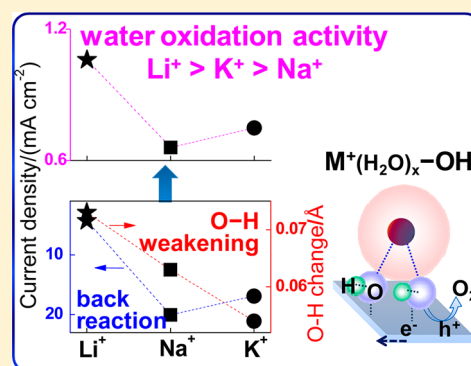
INTRODUCTION

Photoelectrochemical (PEC) water splitting for solar fuel production has been regarded as a promising artificial photosynthesis strategy for future carbon-neutral, storable, and sustainable energy.[1−5] Photogenerated charge carriers must survive from various recombination processes particularly at the electrode−electrolyte interface before being used for the water splitting reaction. Therefore, the engineering of the electrode−electrolyte interface is highly important, even crucial, for enhancing PEC performances. At one side of the interface, the electrode surface has been modified with cocatalyst or other functional species[6−15] to improve its PEC properties. At the other side of the interface, the electrolyte is also essential. The influences of electrolyte species on the water splitting reaction, however, have not been well-studied.

It has been reported that anion species in the electrolyte can remarkably influence the performances of water oxidation (WO) electrocatalysts,[16−18] photocatalyst,[19,20] and cocatalyst/photoanode[21−24] via affecting proton coupled electron transfer,[17,25] structures of catalysts,[18,23] or undergoing self-oxidation reactions.[22,26] Then, how about cation species? In natural photosynthesis, the cationic environment of surface groups can affect the electron transfer steps during WO and quinone reduction reactions in the photosystem-II.[27] Several studies have revealed that the rates of oxygen reduction reaction (ORR), hydrogen oxidation reaction (HOR), methanol oxidation, and CO oxidation on Pt electrode are impacted by the presence of different cations, and Li+ shows the lowest activity for ORR, HOR, methanol oxidation, and the highest activity for CO oxidation compared with other alkaline-metal cations.[28−30] Similarly, the hydrogen evolution activity on the Pt−Ni(OH)$_x$ electrode can also be enhanced via Li+ addition.[31] Besides, in dye-sensitized solar cells, it has been proved that Li+ has strong adsorption on TiO$_2$ and can accelerate the electron injection process.[32−35] Electrolytes with various cations were also found to influence the photocatalytic water splitting activity, but the mechanism was unclear and was supposed that the electrolyte might facilitate surface redox reactions or compensate for surface defects.[36,37] It was reported that the highest WO efficiency was obtained for WO$_3$ photoanode with K+ in acidic electrolytes and the lowest with Li+, which was inferred to be caused by the strongest adsorption of Li+ on the electrode blocking the WO active sites.[38,39] While in other reports, Li+ was suggested to be favorable for WO on Ni-(hydro)oxide catalysts by influencing phase transformation.[11,40] In a word, there remains much controversy about the effects of cations in the electrolyte. Understanding of this issue may shed light on the complicated processes of water splitting and be helpful to develop new strategies to promote the reaction.

Herein, we focus on the effects of cations on the WO reaction. It is found that the photocurrents of (cocatalyst)/TiO$_2$ electrodes in strong alkaline electrolytes decrease in

sequence: LiOH > KOH > NaOH. And the activities of (cocatalyst)/BiVO$_4$ electrodes in medium basic borate electrolytes (pH 9) show a similar trend of (Li$^+$ ∼ K$^+$) > Na$^+$. In accordance, the electrocatalytic activities on the electrodes of the cocatalysts above are consistent with PEC results. The rates of ORR in different electrolytes show an order of Li$^+$ < K$^+$ < Na$^+$, and theoretical calculations show that the strength of the interaction between cations and OH species on the electrode surface follows a sequence of Li$^+$ > Na$^+$ > K$^+$. These two factors are important for the reaction at the electrode−electrolyte interface, while their contributions are not parallel thus resulting in the abnormal trend of WO activity.

■ RESULTS AND DISCUSSION

We investigated the PEC performances of photoanodes in strong alkaline (NaOH, pH 13.6; LiOH, pH 12; NaLiOH, pH 13.1; and KOH, pH 13.9) and alkaline−metal borate electrolytes (pH 9, denoted as LiBi, KBi, NaLiBi, and NaBi). Co-borate (CoBi), Ni-borate (NiBi), ferrihydrite (FeOH), Co$_3$O$_4$, and MnO$_x$ were used as cocatalysts. Employing TiO$_2$-based photoanodes as model electrodes in strong alkaline electrolytes, Figure 1 shows that the photocurrents of bare
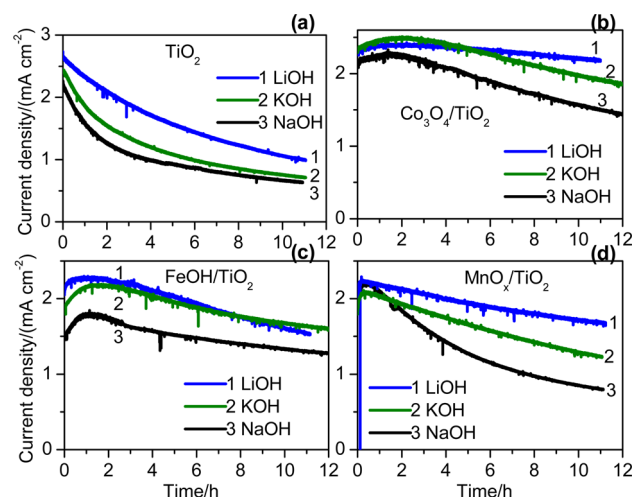

Figure 2. Linear sweep voltammetric curves of (a) TiO$_2$, (b) Co$_3$O$_4$/TiO$_2$, (c) FeOH/TiO$_2$, and (d) MnO$_x$/TiO$_2$ electrodes in 1 M NaOH (pH 13.6), LiOH (pH 12), and KOH (pH 13.9) electrolytes. Light source: 300 W Xe lamp (300 mW cm^{-2}). Scan rate: 50 mV s^{-1}.

curves of (cocatalyst)/TiO$_2$ electrode varies a little for different cases of cocatalysts. Because the surfaces of electrodes are exposed with uncovered TiO$_2$ and cocatalysts, they have different but similar electrode−electrolyte interfaces. But all of them show a common trend of activity: LiOH > KOH > NaOH.

Next, we studied BiVO$_4$-based photoanodes in medium basic borate electrolytes. Figure 3 shows that the photocurrents of bare and cocatalyst (CoBi, NiBi, FeOH, or Co$_3$O$_4$)-modified

Figure 1. I−t curves of (a) TiO$_2$, (b) Co$_3$O$_4$/TiO$_2$, (c) FeOH/TiO$_2$, and (d) MnO$_x$/TiO$_2$ electrodes at 1.23 V vs RHE in 1 M NaOH (pH 13.6), LiOH (pH 12), and KOH (pH 13.9) electrolytes under continuous illumination for 12 h. Light source: 300 W Xe lamp (300 mW cm^{-2}).

TiO$_2$ and cocatalyst (Co$_3$O$_4$, FeOH, or MnO$_x$) modified TiO$_2$ electrodes under long time irradiation in various electrolytes decrease in the order of LiOH > KOH > NaOH. The steady state activities in LiOH and KOH electrolytes are much higher than that in NaOH. In accordance, the initial linear sweep voltammetric (LSV) currents (Figure 2) also show the same order. For the bare TiO$_2$ electrode, the activity difference is observable only in the high potential regime. But for cocatalyst/TiO$_2$, along with higher photocurrent, the onset potential is negatively shifted by 70 mV ∼ 230 mV in LiOH electrolyte compared with that in NaOH. It is supposed that the effects of cations on the onset potential of WO photocurrents mainly stem from the influences on cocatalysts, consistent with the results of electrocatalytic water splitting which will be discussed below. Likewise, the Fe$_2$O$_3$ photoanode shows similar results, namely, the highest activity in LiOH (Figure S1 of the Supporting Information). It is worth mentioning that the LSV
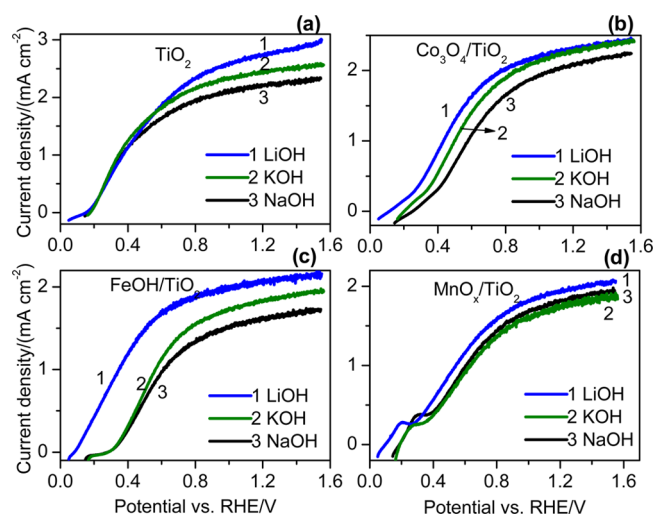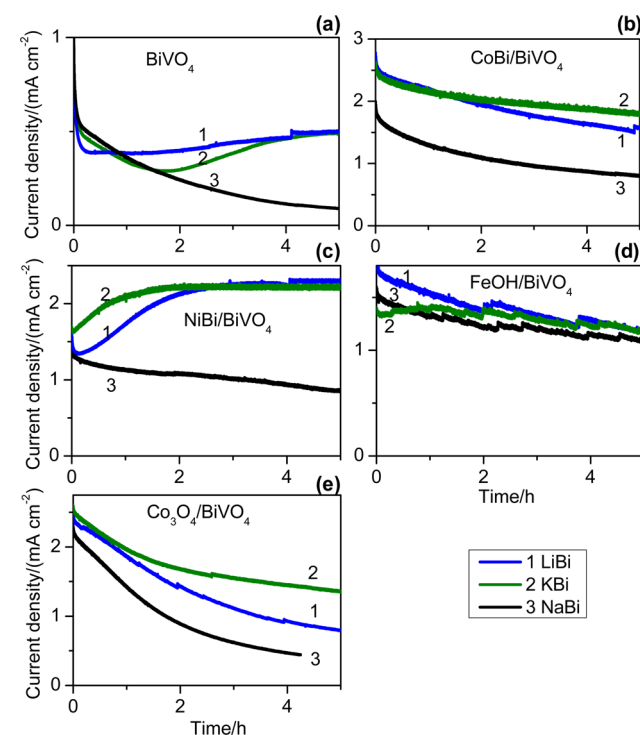

Figure 3. I−t curves of (a) bare BiVO$_4$, (b) CoBi/BiVO$_4$, (c) NiBi/BiVO$_4$, (d) FeOH/BiVO$_4$, and (e) Co$_3$O$_4$/BiVO$_4$ at 1.23 V vs RHE in LiBi, KBi, and NaBi (borate ions 0.5 M, pH 9) electrolytes under continuous irradiation in 5 h. Light source: 300 W Xe lamp (λ > 420 nm, 300 mW cm^{-2}).

BiVO$_4$ electrodes under long time irradiation in borate electrolytes follow a trend of (LiBi ~ KBi) > NaBi. The activities in LiBi and KBi electrolytes are more stable over time, while the photocurrent in NaBi decays quickly. Especially for CoBi and NiBi cocatalysts, the stability difference is significant. There are also slight activity differences in the initial LSV photocurrents (Figure S2 of the Supporting Information), but the shifts of the onset potential are negligible, which is different from that in the strong basic electrolytes.

To reveal the reasons for the PEC activity difference, we assessed the electrocatalytic WO using the cocatalysts above as electrodes in various electrolytes. Figure 4 shows that the initial
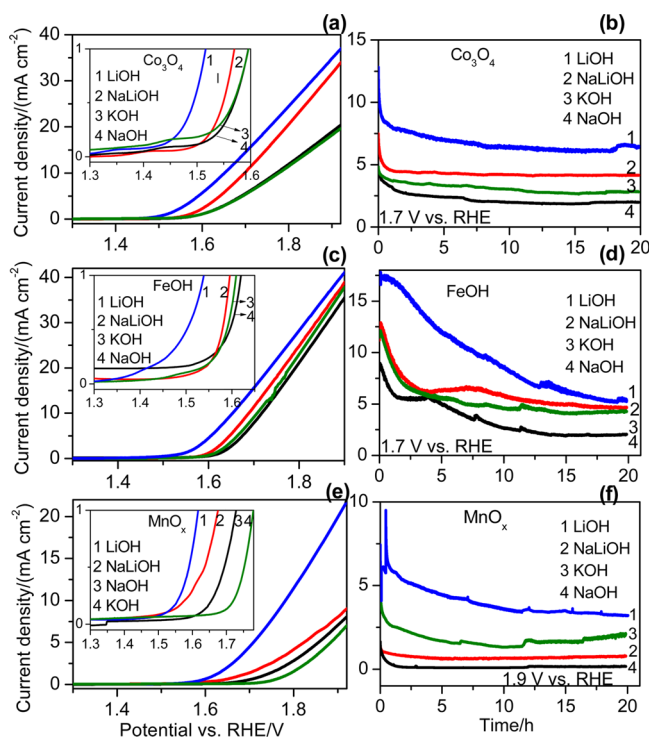

Figure 4. Linear sweep voltammetric curves and corresponding I−t curves of (a, b) Co$_3$O$_4$ at 1.7 V vs RHE, (c, d) FeOH at 1.7 V vs RHE, and (e, f) MnO$_x$ at 1.9 V vs RHE in 1 M NaOH (pH 13.6), LiOH (pH 12), KOH (pH 13.9), and NaLiOH (0.8 M NaOH and 0.2 M LiOH, pH 13.13) electrolytes for 20 h. Insets are the amplified plots of (a, c, and e) near the onset potential. Scan rate: 20 mV s^{-1}.

LSV and I−t currents of Co$_3$O$_4$, FeOH, and MnO$_x$ electrodes in the LiOH electrolyte are obviously higher than those in KOH, NaLiOH, and NaOH. Besides, the onset potential in the LiOH electrolyte is negatively shifted by about 100 mV compared with that in NaOH. The extent of onset potential shift and activity difference vary in different cases of catalysts, but all show the same trend: LiOH > KOH > NaOH in consistence with the PEC results above. This result further indicates that the PEC activity difference are mainly contributed by the distinct performances of cocatalysts in different electrolytes.

In the case of borate electrolytes, the electrocatalytic activities in LiBi and KBi are generally higher than that in the NaBi electrolyte, consistent with the PEC results in Figure 3. Figure 5 indicates the currents over time show an order of (LiBi ~ KBi) > NaLiBi > NaBi for NiBi and FeOH electrodes, and the trend is LiBi > NaLiBi > KBi > NaBi for CoBi and Co$_3$O$_4$. The current fluctuation is caused by disturbance of the system from
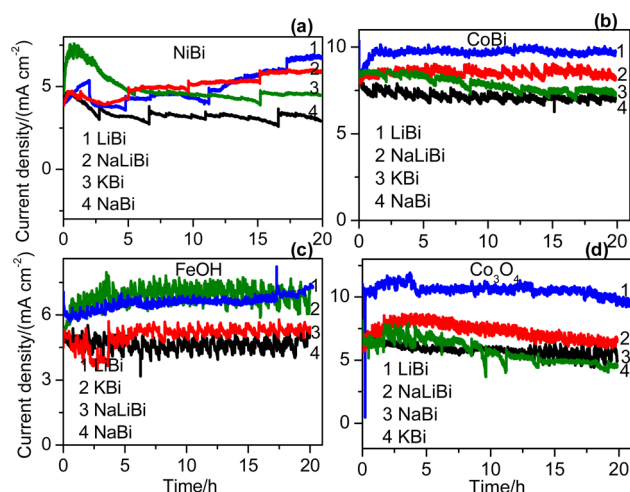

Figure 5. I−t curves of (a) NiBi, (b) CoBi, (c) FeOH, and (d) Co$_3$O$_4$ electrodes in LiBi, KBi, NaLiBi, and NaBi (borate ions 0.5 M, pH 9) electrolytes at 1.9 V vs RHE in 20 h.

bubbles produced at the electrode. Activities of in situ electrocatalytic WO in electrolytes containing Co^{2+} and Ni^{2+} are also higher in LiBi and KBi electrolytes than that in NaBi (Figure S3 of the Supporting Information). Besides, it is notable that the activity difference in weak basic electrolytes is more obvious for a long time reaction, while the initial activity in LiBi is only slightly higher or nearly the same with those in KBi and NaBi electrolytes (Figure S4 of the Supporting Information), probably as it takes some time to reach a steady state of electrolyte−electrode interface or some important factors are more significant during a long time reaction.

Thus, it can be concluded that the PEC and electrocatalytic WO activities in basic electrolytes with different cations decrease in the sequence: Li$^+$ > K$^+$ > Na$^+$, especially for long time reaction. But what is the essential reason behind the phenomenon?

Table 1 lists the solution resistances (Rs) of a FTO electrode in borate and strong alkaline electrolytes. There are negligible

Table 1. Solution Resistances (Rs) of Different Electrolytes Measured in a Three-Electrode System with a FTO as Working Electrode

electrolyte	Rs (Ω cm^{-2})	electrolyte	Rs (Ω cm^{-2})
NaBi	48.3	NaOH	30.6
NaLiBi	49.1	NaLiOH	30.6
KBi	47.0	KOH	31.2
LiBi	53.6	LiOH	30.3

differences among electrolytes with different cations, indicating that the conductivity of the electrolyte is not the reason for the activity difference.

It has been well-proved that the WO reaction in basic condition involves O−H bond dissociation processes which are usually slow.[41,42] Previous reports[28−31] show that hydrated cations M$^+$(H$_2$O)$_x$ (x denotes the hydration number) can interact with OH species adsorbed on the electrode forming complexes like electrode−OH−M$^+$(H$_2$O)$_x$ through noncovalent interactions, including hydrogen bond and electrostatic interactions as depicted in Figure 6a. Such complexes can enhance the adsorption of OH species and block the active sites for O$_2$ and H$_2$ adsorption,[28−30] which will inhibit ORR and
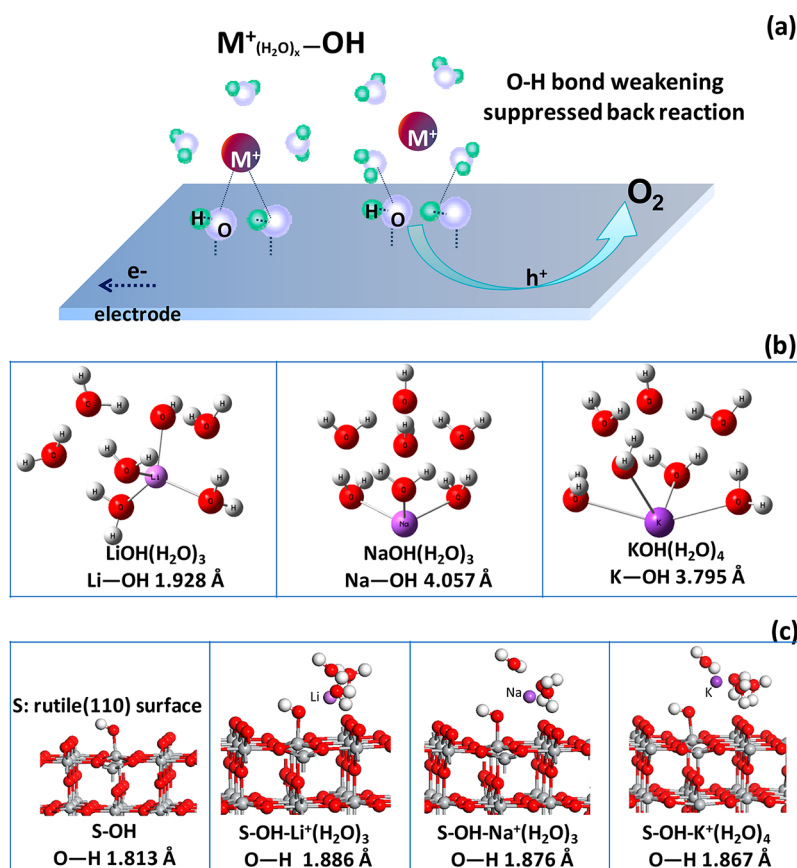
Figure 6. (a) Schematic description of the effect on water oxidation of the interaction between hydrated cations and OH species on the electrode surface, theoretical calculation results of (b) the optimized structures of free alkali-metal hydroxides clusters $MOH(H_2O)_x$ (M = Li, Na, and K) and the average distance between M^+ and OH^-, (c) the change of O—H bond on rutile (110) surface before and after its interaction with hydrated cations in the electrolyte [coloring scheme: red (O atoms), gray (Ti atoms), purple (Li, Na, and K atoms), and white (H atoms)].

induce the weakening of the O—H bond.[31] Could that be the cause of the WO activity difference?

To gain more insight, density functional theory (DFT) calculations were performed. We used alkali-metal hydroxides hydrated by six water molecules, $MOH(H_2O)_6$ (M = Li, Na, and K), to simulate free hydrated cations. The initial geometries of $MOH(H_2O)_6$ were taken from the most stable structures in previous reports.[43,44] The calculated results in Figure 6b suggest that the number of water molecule bonding to alkali-metal cation is three for Li^+, three for Na^+, and four for K^+. Interestingly, the distances between M^+ and OH^- increase in a sequence of Li^+(1.928 Å) < K^+(3.795 Å) < Na^+(4.057 Å). In the real reaction conditions, however, hydrated cations were not totally free. So in order to mimic the experimental environment, we carried out first-principle DFT calculations of hydrated cations rutile TiO_2 (110) surface adsorbed with OH species. The number of water molecule around alkali-metal cations was set to three for Li^+, three for Na^+, and four for K^+ generated from the optimized structures of the free hydrated cations. Figure 6c displays the changes of the O—H bond adsorbed on the rutile (110) surface before and after interacting with the hydrated cations. The length of O—H bond increases from 1.813 to 1.886 Å, 1.876 Å, and 1.867 Å after interacting with $Li^+(H_2O)_3$, $Na^+(H_2O)_3$, $K^+(H_2O)_4$ cations, respectively. In other words, the strength of the interaction between hydrated cations and OH species on the electrode surface and the extent of O—H bond weakening follow a trend of $Li^+ > Na^+ > K^+$. Previous works have also revealed that the adsorption of

Li^+ on metal oxide such as TiO_2, Fe_2O_3, and WO_3 is much stronger than other alkaline-metal ions.[32−35,39,45] And this effect may not only affect the initial WO activity and onset potential but also the performance of the electrode under the long time reaction because the interaction between cations and the electrode is there as long as the electrode−electrolyte interface is formed. These analyses lead us to deduce that the difference of WO activities in various electrolytes is partly due to the different extent of O−H bond weakening caused by the interaction of cations with OH species on the electrode surface.

But, the effect of the weakening O−H bond cannot fully account for the WO activity difference and cannot explain why K^+ is better than Na^+. So there must be some additional effects of cations. It is reported that K^+ has the most significant perturbation effect on the structure of water clusters at the silica surface, with a trend of $K^+ > Li^+ > Na^+$.[46] The perturbation may be helpful for the mass transfer near the electrode surface and beneficial to WO reaction, which could be a possible explanation for the phenomena that K^+ gives higher activity than Na^+, but more detailed research must be addressed.

It was reported that the water splitting reaction on particle photocatalysts was facilitated when the ORR on surface was suppressed by introducing O_2 nonpermeable oxyhydroxide layers.[47−49] And in PEC water splitting, previous research has also proved that the performances of Fe_2O_3[6] and $BiVO_4$[50] photoanodes can be dramatically enhanced after suppressing ORR via surface treatment. Therefore, back reaction may be an important factor influencing the WO activity of a photoanode.

In our work, although the electrolyte was bubbled with Ar gas during electrochemical measurements, it was observed that O_2 can still accumulate into small bubbles adhered to the electrode which can cause back reaction. Thus, the distinct rates of ORR should be another important reason for the WO activity difference in different electrolytes, especially when the applied potential is not so positive and during a long time reaction. Figure 7 shows the ORR activities of inert electrodes in
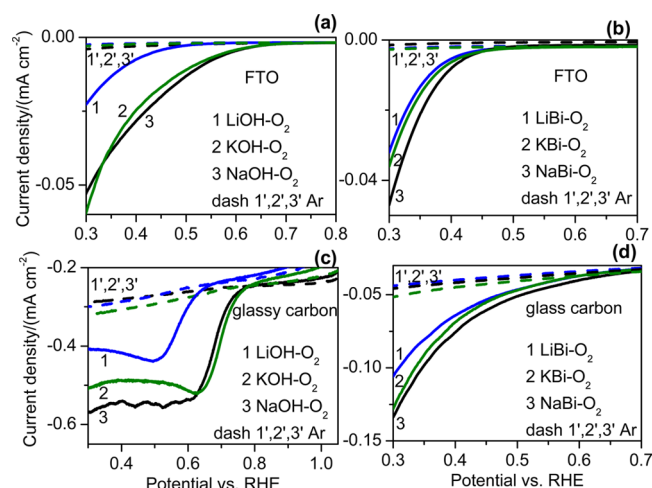

Figure 7. Linear sweep voltammetric reduction currents on (a and b) blank FTO electrode and (c and d) glassy carbon electrode in 1 M NaOH (pH 13.6), LiOH (pH 12), and KOH (pH 13.9) electrolytes and LiBi, NaBi, and KBi (borate ions 0.5 M, pH 9) electrolytes presaturated with Ar (dashed lines) and O_2 (solid lines) for 15 min. Scan rate: 20 mV s^{-1}.

electrolytes with different cations. There are little differences when the electrolytes are saturated with Ar. However, in electrolytes presaturated with O_2, the ORR currents demonstrate a trend of Li$^+$ < K$^+$ < Na$^+$. This is nearly the reverse order of WO activity. To be more confident about the results, two kinds of electrodes (blank FTO and glassy carbon) were used as working electrodes, and the same trend was obtained both in strong alkaline and medium basic electrolytes. The similar trend about the cation dependence of ORR activity on Pt electrode has also been reported in the literature.[28]

Therefore, given the above findings, it is reasonable to conclude that Li$^+$ not only shows the most significant effect of O−H bond destabilization but also is most effective for avoiding back reaction, while Na$^+$ shows the most detrimental effects on PEC WO because of ORR. In other words, the final abnormal cation dependence of WO activity (Li$^+$ > K$^+$ > Na$^+$) is the balance effect of mainly two factors: one is the different extents of O−H bond weakening caused by the interaction of various cations with OH on the electrode surface and the other, probably the dominant, is the distinct rates of surface ORR in different electrolytes.

CONCLUSION

It is found that the WO activities of (cocatalyst)/TiO$_2$ photoelectrodes in strong alkaline electrolytes show a trend of LiOH > KOH > NaOH with obvious cathodic shift of onset potential, and the photocurrents of (cocatalyst)/BiVO$_4$ electrodes in borate electrolytes (pH 9) follow a general order of (LiBi ∼ KBi) > NaBi during the long time reaction. The electrocatalytic WO activities in the dark condition are

consistent with the PEC results. Such an abnormal trend of WO activity is the net effects of mainly two factors: one is the different extent of O−H bond weakening caused by the interaction of various cations with OH species on the electrode surface, the other factor which turns out to be dominant is the different rates of surface ORR in various electrolytes. Li$^+$ shows the most significant extent of O−H bond weakening and is most effective for avoiding back reaction, while Na$^+$ shows the most detrimental effect on WO because of ORR.

ASSOCIATED CONTENT

Ⓢ Supporting Information

Details about chemicals and materials, preparation of the electrolytes, fabrication of electrodes, (photo)electrochemical characterizations, characterizations and electrochemical measurements, computational methods, $I-t$ curves (Figures S1 and S3), linear sweep voltammetric curves (Figures S2 and S4), XRD patterns (Figure S5), and the activities of photoanode before and after loading cocatalyst (Figures S6 and S7). This material is available free of charge via the Internet at http://pubs.acs.org.

AUTHOR INFORMATION

Corresponding Author
*E-mail: canli@dicp.ac.cn. Tel: 86-411-84379070. Fax: 86-411-84694447. Homepage: http://www.canli.dicp.ac.cn.

Notes
The authors declare no competing financial interest.

REFERENCES

(1) Chen, Z. B.; Jaramillo, T. F.; Deutsch, T. G.; Kleiman-Shwarscstein, A.; Forman, A. J.; Gaillard, N.; Garland, R.; Takanabe, K.; Heske, C.; Sunkara, M.; et al. Accelerating materials development for photoelectrochemical hydrogen production: Standards for methods, definitions, and reporting protocols. *J. Mater. Res.* 2010, 25 (1), 3−16.

(2) Li, Z.; Luo, W.; Zhang, M.; Feng, J.; Zou, Z. Photoelectrochemical cells for solar hydrogen production: current state of promising photoelectrodes, methods to improve their properties, and outlook. *Energy Environ. Sci.* 2013, 6, 347−370.

(3) Park, Y.; McDonald, K. J.; Choi, K. Progress in bismuth vanadate photoanodes for use in solar water oxidation. *Chem. Soc. Rev.* 2013, 42, 2321−2337.

(4) Abe, R. Recent progress on photocatalytic and photoelectrochemical water splitting under visible light irradiation. *J. Photochem. Photobiol. C* 2010, 11 (4), 179−209.

(5) Walter, M. G.; Warren, E. L.; McKone, J. R.; Boettcher, S. W.; Mi, Q.; Santori, E. A.; Lewis, N. S. Solar water splitting cells. *Chem. Rev.* 2010, 110 (11), 6446−6473.

(6) Cao, D.; Luo, W.; Feng, J.; Zhao, X.; Li, Z.; Zou, Z. Cathodic shift of onset potential for water oxidation on a Ti^{4+} doped Fe$_2$O$_3$ photoanode by suppressing back reaction. *Energy Environ. Sci.* 2014, 7, 752−759.

(7) Yang, J.; Walczak, K.; Anzenberg, E.; Toma, F. M.; Yuan, G.; Beeman, J.; Schwartzberg, Adam; Lin, Y.; Hettick, M.; Javey, A.; Ager, J. W.; Yano, J.; Frei, H.; Sharp, I. D. Efficient and Sustained Photoelectrochemical Water Oxidation by Cobalt Oxide/Silicon Photoanodes with Nanotextured Interfaces. *J. Am. Chem. Soc.* **2014**, *136* (17), 6191−6194.

(8) Tilley, S. D.; Schreier, M.; Azevedo, J.; K, M. S.; Graetzel, M. Ruthenium Oxide Hydrogen Evolution Catalysis on Composite Cuprous Oxide Water-Splitting Photocathodes. *Adv. Funct. Mater.* **2013**, *24* (3), 303−311.

(9) Hou, J.; Yang, C.; Wang, Z.; Cheng, H.; Jiao, S.; Zhu, H. Cobalt-bilayer catalyst decorated Ta3N5 nanorod arrays as integrated electrodes for photoelectrochemical water oxidation. *Energy Environ. Sci.* **2013**, *6* (11), 3322−3330.

(10) Seger, B.; Pedersen, T.; Laursen, A. B.; Vesborg, P. C. K.; Hansen, O.; Chorkendorff, I. Using TiO2 as a Conductive Protective Layer for Photocathodic H2 Evolution. *J. Am. Chem. Soc.* **2013**, *135*, 1057−1064.

(11) Kenney, M. J.; Gong, M.; Li, Y.; Wu, J. Z.; Feng, J.; Lanza, M.; Dai, H. High-Performance Silicon Photoanodes Passivated with Ultrathin Nickel Films for Water Oxidation. *Science* **2013**, *342* (6160), 836−840.

(12) Pilli, S. K.; Furtak, T. E.; Brown, L. D.; Deutsch, T. G.; Turner, J. A.; Herring, A. M. Cobalt-phosphate (Co-Pi) catalyst modified Mo-doped BiVO4 photoelectrodes for solar water oxidation. *Energy Environ. Sci.* **2011**, *4* (12), 5028−5034.

(13) Liu, R.; Zheng, Z.; Spurgeon, J.; Brunschwig, B. S.; Yang, X. Enhanced Photoelectrochemical Water-Splitting Performance of Semiconductors by Surface Passivation Layers. *Energy Environ. Sci.* **2014**, *7*, 2504−2517.

(14) Kim, J. Y.; Jang, J.; Youn, D. H.; Magesh, Ganesan; Lee, J. S. Stable and efficient hematite photoanode in neutral electrolyte for solar water splitting: Towards stability engineering. *Adv. Energy Mater.* **2014**, *4* (1400476), 1−7.

(15) Li, M.; Luo, W.; Cao, D.; Zhao, X.; Li, Z.; Yu, T.; Zou, Z. A Cocatalyst-Loaded Ta3N5 Photoanode with a High Solar Photo-current for Water Splitting upon Facile Removal of the Surface Layer. *Angew. Chem., Int. Ed.* **2013**, *52*, 1−6.

(16) Lutterman, D. A.; Surendranath, Y.; Nocera, D. G. A Self-Healing Oxygen-Evolving Catalyst. *J. Am. Chem. Soc.* **2009**, *131* (11), 3838−3839.

(17) Surendranath, Y.; Dincă, M.; Nocera, D. G. Electrolyte-Dependent Electrosynthesis and Activity of Cobalt-Based Water Oxidation Catalysts. *J. Am. Chem. Soc.* **2009**, *131* (7), 2615−2620.

(18) Risch, M.; Klingan, K.; Ringleb, F.; Chernev, P.; Zaharieva, I.; Fischer, A.; Dau, H. Water Oxidation by Electrodeposited Cobalt Oxides—Role of Anions and Redox-Inert Cations in Structure and Function of the Amorphous Catalyst. *ChemSusChem* **2012**, *5* (3), 542−549.

(19) Miseki, Y.; Kusama, H.; Sugihara, H.; Sayama, K. Significant Effects of Anion in Aqueous Reactant Solution on Photocatalytic O2 Evolution and Fe(III) Reduction. *Chem. Lett.* **2010**, *39*, 846−847.

(20) Sayarna, K.; Arakawa, H. Effect of carbonate addition on the photocatalytic decomposition of liquid water over a ZrO2 catalyst. *J. Photochem. Photobiol., A* **1996**, *94*, 67−76.

(21) Liao, M.; Feng, J.; Luo, W.; Wang, Z.; Zhang, J.; Li, Z.; Yu, T.; Zou, Z. Co3O4 Nanoparticles as Robust Water Oxidation Catalysts Towards Remarkably Enhanced Photostability of a Ta3N5 Photo-anode. *Adv. Funct. Mater.* **2012**, *22* (14), 3066−3074.

(22) Mi, Q.; Coridan, R. H.; Brunschwig, B. S.; Gray, H. B.; Lewis, N. S. Photoelectrochemical oxidation of anions by WO3 in aqueous and nonaqueous electrolytes. *Energy Environ. Sci.* **2013**, *6* (9), 2646−2653.

(23) Higashi, M.; Domen, K.; Abe, R. Highly Stable Water Splitting on Oxynitride TaON Photoanode System under Visible Light Irradiation. *J. Am. Chem. Soc.* **2012**, *134* (16), 6968−6971.

(24) Ding, C.; Shi, J.; Wang, D.; Liu, G.; Xiong, F.; Li, C. Visible light driven overall water splitting using cocatalyst/BiVO4 photoanode with minimized bias. *Phys. Chem. Chem. Phys.* **2013**, *15*, 4589−4595.

(25) Bediako, D. K.; Costentin, C.; Jones, E. C.; Nocera, D. G.; Saveant, J. Proton-Electron Transport and Transfer in Electrocatalytic Films. Application to a Cobalt-Based O2-Evolution Catalyst. *J. Am. Chem. Soc.* **2013**, *135* (28), 10492−10502.

(26) Mi, Q.; Zhanaidarova, A.; Brunschwig, B. S.; Gray, H. B.; Lewis, N. S. A quantitative assessment of the competition between water and anion oxidation at WO3 photoanodes in acidic aqueous electrolytes. *Energy Environ. Sci.* **2012**, *5* (2), 5694−5700.

(27) Karge, O.; Bondar, A. N.; Dau, H. Cationic screening of charged surface groups (carboxylates) affects electron transfer steps in photosystem-II water oxidation and quinone reduction. *Biochim. Biophys. Acta* **2014**, *1837* (10), 1625−1634.

(28) Strmcnik, D.; Escudero-Escribano, M.; Kodama, K.; Stamenkovic, V. R.; Cuesta, A.; Markovic, N. M. Enhanced electrocatalysis of the oxygen reduction reaction based on patterning of platinum surfaces with cyanide. *Nat. Chem.* **2010**, *2* (10), 880−885.

(29) Strmcnik, D.; Kodama, K.; van der Vliet, D.; Greeley, J.; Stamenkovic, V. R.; Markovic, N. M. The role of non-covalent interactions in electrocatalytic fuel-cell reactions on platinum. *Nat. Chem.* **2009**, *1* (6), 466−472.

(30) Stoffelsma, C.; Rodriguez, P.; Garcia, G.; Garcia-Araez, N.; Strmcnik, D.; Markovic, N. M.; Koper, M. T. M. Promotion of the Oxidation of Carbon Monoxide at Stepped Platinum Single-Crystal Electrodes in Alkaline Media by Lithium and Beryllium Cations. *J. Am. Chem. Soc.* **2010**, *132* (45), 16127−16133.

(31) Subbaraman, R.; Tripkovic, D.; Strmcnik, D.; Chang, K.; Uchimura, M.; Paulikas, A. P.; Stamenkovic, V.; Markovic, N. M. Enhancing Hydrogen Evolution Activity in Water Splitting by Tailoring Li+-Ni(OH)2-Pt Interfaces. *Science* **2011**, *334* (6060), 1256−1260.

(32) Meyer, D. F. W. G. Cation effects in nanocrystalline solar cells. *Coord. Chem. Rev.* **2004**, *248* (13−14), 1391−1406.

(33) Zhang, C.; Huo, Z.; Huang, Y.; Dai, S.; Wang, M.; Tang, Y.; Sui, Y. Electrolyte effects on photoelectron injection and recombination dynamics in dye-sensitized solar cells. *J. Photochem. Photobiol., A* **2010**, *213*, 87−92.

(34) Zhang, C.; Dai, J.; Huo, Z.; Pan, X.; Hu, L.; Kong, F.; Huang, Y.; Sui, Yifeng; Fang, X. KongjiaWang; Dai, S. Influence of 1-methylbenzimidazole interactions with Li+ and TiO2 on the perform-ance of dye-sensitized solar cells. *Electrochim. Acta* **2008**, *53* (17), 5503−5508.

(35) Thompson, D. W.; Kelly, C. A.; Farzad, F.; Meyer, G. J. Sensitization of nanocrystalline TiO2 initiated by reductive quenching of molecular excited states. *Langmuir* **1999**, *15* (3), 650−653.

(36) Maeda, K.; Masuda, H.; Domen, K. Effect of electrolyte addition on activity of (Ga1-xZnx)(N1-xOx) photocatalyst for overall water splitting under visible light. *Catal. Today* **2009**, *147* (3−4SI), 173−178.

(37) Ji, S. M.; Jun, H.; Jang, J. S.; Son, H. C.; Borse, P. H.; Lee, J. S. Photocatalytic hydrogen production from natural seawater. *J. Photo-chem. Photobiol., A* **2007**, *189* (1), 141−144.

(38) Hill, J. C.; Choi, K. Effect of Electrolytes on the Selectivity and Stability of n-type WO3 Photoelectrodes for Use in Solar Water Oxidation. *J. Phys. Chem. C* **2012**, *116* (14), 7612−7620.

(39) YAT, D. E.; HEAL, T. W. Titanium dioxide/electrolyte solution interface: Part 2.-Surface Charge (Titration) Studies. *J. Chem. Soc., Faraday Trans.* **1980**, *76*, 9−18.

(40) Tuomi, D. The Forming Process in Nickel Positive Electrodes. *J. Electrochem. Soc.* **1965**, *112* (1), 1−12.

(41) Fang, Y.; Liu, Z. Mechanism and Tafel Lines of Electro-Oxidation of Water to Oxygen on RuO2(110). *J. Am. Chem. Soc.* **2010**, *132* (51), 18214−18222.

(42) Zhao, W.; Liu, Z. Mechanism and active site of photocatalytic water splitting on titania in aqueous surroundings. *Chem. Sci.* **2014**, *5* (6), 2256−2264.

(43) Veerman, A.; Lee, H. M.; Kim, K. S. Dissolution nature of the lithium hydroxide by water molecules. *J. Chem. Phys.* **2005**, *123* (0843218), 843211−843217.

(44) Kumar, A.; Park, M.; Huh, J. Y.; Lee, H. M.; Kim, K. S. Hydration phenomena of sodium and potassium hydroxides by water molecules. *J. Chem. Phys. A* **2006**, *110* (45), 12484−12493.

(45) Creux, P.; Lachaise, J.; Graciaa, A.; Beattie, J. K. Specific cation effects at the hydroxide-charged air/water interface. *J. Phys. Chem. C* **2007**, *111* (9), 3753−3755.

(46) Yang, Z.; Li, Q.; Chou, K. C. Structures of Water Molecules at the Interfaces of Aqueous Salt Solutions and Silica: Cation Effects. *J. Phys. Chem. C* **2009**, *113* (19), 8201−8205.

(47) Pan, C.; Takata, T.; Nakabayashi, M.; Matsumoto, T.; Shibata, N.; Ikuhara, Y.; Domen, K. A Complex Perovskite-Type Oxynitride: The First Photocatalyst for Water Splitting Operable at up to 600 nm. *Angew. Chem., Int. Ed.* **2015**, *54*, 1−6.

(48) Maeda, K.; Sakamoto, N.; Ikeda, T.; Ohtsuka, H.; Xiong, A. K.; Lu, D. L.; Kanehara, M.; Teranishi, T.; Domen, K. Preparation of Core-Shell-Structured Nanoparticles (with a Noble-Metal or Metal Oxide Core and a Chromia Shell) and Their Application in Water Splitting by Means of Visible Light. *Chem.—Eur. J.* **2010**, *16* (26), 7750−7759.

(49) Yoshida, M.; Takanabe, K.; Maeda, K.; Ishikawa, A.; Kubota, J.; Sakata, Y.; Ikezawa, Y.; Domen, K. Role and Function of Noble-Metal/ Cr-Layer Core/Shell Structure Cocatalysts for Photocatalytic Overall Water Splitting Studied by Model Electrodes. *J. Phys. Chem. C* **2009**, *113* (23), 10151−10157.

(50) Eisenberg, D.; Ahn, H. S.; Bard, A. J. Enhanced photo-electrochemical water oxidation on bismuth vanadate by electro-deposition of amorphous titanium dioxide. *J. Am. Chem. Soc.* **2014**, *136*, 14011−14014.

G